

DR. ANDREW S JONES (Orcid ID : 0000-0002-0995-4957)

Article type : Technical Paper

Use of Predictive Weather Uncertainties in an Irrigation Scheduling Tool Part II: An Application of Metrics and Adjoint

Andrew S. Jones, Allan A. Andales, José L. Chávez, Cullen McGovern, Garvey E. B. Smith,
Olaf David, and Steven J. Fletcher

Cooperative Institute for Research in the Atmosphere (**Jones, Fletcher**), Department of Soil and Crop Sciences (**Andales, McGovern, Smith**), and Department of Civil and Environmental Engineering (**Chávez, David**), Colorado State University, Fort Collins, Colorado, USA (Correspondence to Jones: Andrew.S.Jones@ColoState.edu).

Research Impact Statement: Quantitative precipitation forecast data, verification metrics, and adjoint sensitivities are applied to advance the quality of irrigation scheduling tools.

ABSTRACT: We apply predictive weather metrics and land model sensitivities to improve the Colorado State University Water Irrigation Scheduler for Efficient Application (WISE). WISE is an irrigation decision aid that integrates environmental and user information for optimizing water use. Rainfall forecasts and verification performance metrics are used to estimate predictive rainfall probabilities that are used as input data within the irrigation decision aid. These input data errors are also used within a land model sensitivity study to diagnose important prognostic water movement behaviors for irrigation tool development purposes simultaneously performing the analysis in space and time. Thus, important questions such as “how long can a crop water

This is the author manuscript accepted for publication and has undergone full peer review but has not been through the copyediting, typesetting, pagination and proofreading process, which may lead to differences between this version and the [Version of Record](#). Please cite this article as doi: [10.1111/1752-1688.12806](https://doi.org/10.1111/1752-1688.12806)

This article is protected by copyright. All rights reserved

application be delayed while maintaining crop yield production?” are addressed by evaluating crop growth stage interactions as a function of soil depth (i.e. space), rainfall events (i.e. time), and their probabilistic uncertainties. *Editor’s note: This paper is part of the featured series on Optimizing Ogallala Aquifer Water Use to Sustain Food Systems. See the February 2019 issue for the introduction and background to the series.*

(KEYWORDS: data assimilation; irrigation; precipitation; soil moisture; statistics.)

INTRODUCTION

The goal of this work is to apply the methods reviewed and introduced in Jones et al. (2019) to specific examples to improve irrigation decision making. The companion paper (Jones et al. 2019) described a set of methods that are necessary to link the probabilistic predictive weather data to the irrigation tool performance and its possible optimization for economic and agricultural productivity. Here we link probabilistic weather performance to the application of the CSU Water Irrigation Scheduler for Efficient Application (WISE) tool (Andales et al., 2014; Bartlett et al., 2015; WISE. Accessed August 19, 2019, <http://wise.colostate.edu/>) using predictive weather data (aWhere, Inc. system. Accessed August 19, 2019: <https://www.aWhere.com>). Forecast metrics are used to assess the predictive rainfall performance and a land model sensitivity study is used to analyze soil moisture profile behaviors. The sensitivity analysis links the weather input data errors in space and time to water movement diagnostics for use in irrigation scheduling improvements.

A follow-on study within the Ogallala Water Coordinated Project (OWCAP) (OWCAP, Accessed, August 19, 2019, <https://www.ogallalawater.org>) is underway utilizing irrigation schedulers within a variety of crop management and irrigation-decision situations, including subsequent crop yield estimates from these tool-based management decisions. A short review of similar irrigation tools to WISE (e.g., Kansas State University’s KanSched (Roger and Alam, 2007); Texas A&M’s Dashboard for Irrigation Efficiency Management (DIEM), Accessed August 19, 2019, <https://diem.tamu.edu/dashboard/content/static/landing/LandingPage.html>) is found in Jones et al. (2019). As applied here, the concepts demonstrate the ability of weather/soil modeling systems to diagnose important prognostic water movement behaviors for use in irrigation tool development and use. Important questions are addressed, such as “how long can a crop water application be delayed while maintaining crop yield production?” by evaluating crop

growth stage interactions as a function of soil depth and rainfall events and their uncertainties. Lastly, we summarize and draw conclusions from these results, and discuss future implications and needs.

METHODOLOGY

In our companion paper (Jones et al., 2019) we reviewed a set of verification metrics for predictive precipitation from the national data center weather models. Here we apply the reviewed probability performance metric methodologies to examine predictive rainfall performance for a specific example. In addition, in our companion paper (Jones et al., 2019) we presented a series of adjoint sensitivity methodologies. Here, after the performance metrics analysis, we demonstrate the adjoint sensitivity methodology applied to a specific space-time analysis example. We focus on the probabilistic sensitivity of the system to the applied water as a function of soil depth and time, as the applied water from a predictive model will also be probabilistic in its estimate of future rainfall. Thus, crop management needs correspond to water consumption requirements at various soil depths related to the potential wait-times of the possible upcoming natural rainfall events. Using the adjoint techniques from Jones et al. (2019), the tradeoff between statistical predictive natural rainfall estimates and irrigation water application management decisions can then be made in a quantitative probabilistic analysis as part of an optimization of a non-linear dynamical system (Fletcher 2017).

Precipitation Forecast Verification Metrics

Performance analysis of irrigation tools using predictive weather data is possible using the Threat Score (TS), Equitable Threat Score (ETS), and Bier Score (BS) probability performance metrics (Jones et al., 2019). For the following simplified examples, only TS is used to demonstrate the use and interpretation of performance metrics within an adjoint sensitivity context. Many other metrics could be similarly used since the adjoint sensitivity methods make use of cost function constraint terms that could be augmented with metric-derived cost term constraints. The Threat Score is defined as a simple ratio of the “hits” to the total number of events:

$$TS = \frac{a}{a + b + c}. \quad (1)$$

where a is the number of “hits”, b is the number of “false alarms”, and c is the number of “misses” (Wilks, 1995). TS performance metrics are in common use for forecasts out to three days (72h). The National Oceanographic and Atmospheric Administration (NOAA) Global Forecast System (GFS) TS scores are available from NOAA/National Center for Environmental Prediction (NCEP) (NOAA/NCEP. Accessed August 19, 2019, <https://www.wpc.ncep.noaa.gov/html/hpcverif.shtml>). Also fundamental to performance is the Frequency Bias metric (also known as FBIAS by some), and is defined as (Wilks, 1995):

$$\text{BIAS} = \frac{a + b}{a + c} , \quad (2)$$

and is the ratio of total rain forecasts (hits and false alarms) to the total number of observations (hits and misses). A perfect score for BIAS would be 1. BIAS is commonly used by the weather community (Novak, 2014).

Details of the NOAA/NCEP Weather Prediction Center (WPC) verification metrics and performance are discussed in Novak et al. (2014), with related land surface model performance discussed in Xia et al. (2015). It is important to note that WPC monthly TS and BIAS metrics are reported for 24h precipitation forecast TS scores for: Day 1 (24 h), Day 1-update, Day 2, and Day 3 forecast periods using 0.5, 1.0, 2.0, and 3.0 in. (1.27, 2.54, 5.14, and 7.62 cm) precipitation thresholds. The various reporting thresholds allow for the consideration of unique precipitation amounts that may be required for irrigation tool management choices, as not all irrigation equipment can complete their full water application cycle in 12 or 24 hours (or longer). Thus, some irrigation schedule tool users may require additional flexibility to note how much water would be meaningful to their particular irrigation decisions and water throughput capacities.

In addition to the TS and BIAS information, the WPC creates monthly composited sets of Brier Score (BS) values for the medium-range probability of precipitation (PoP) forecasts in the 3-7 day forecast range (Weather Prediction Center, Accessed August 19, 2019, <https://www.wpc.ncep.noaa.gov/html/hpcverif.shtml>). The BS is defined as:

$$\text{BS} = \frac{1}{n} \sum_{k=1}^n (p_k - o_k)^2 , \quad (3)$$

where n is the total number of forecasts, k represents the k th forecast or observation of n total forecasts, and p_k and o_k are the forecast and observed probabilities for each k th forecast, respectively (Brier, 1950).

The need for BS was in part determined by the nature of medium range forecasting, as weather forecasts can be improved substantially by aggregating many models together into the ensemble. Thus, new verification metrics were developed to suit the ensemble nature of the more accurate medium-range PoP predictions (Marty et al., 2012). The ensemble aspect of short and medium range weather prediction continues to undergo rapid advancement which may result in new metrics for precipitation assessment or more advanced post-processing (e.g., Model Output Statistics (MOS)) to minimize known artifacts (Jones et al., 2007; Charba and Samplatsky, 2011; Novak et al., 2014; Hamill et al., 2017); however, the requirement for longterm institutional monitoring of weather forecast improvement makes it likely that key forecast metrics like the TS, BIAS, and BS will be used by the operational centers for the foreseeable future. Of course, new methods and data sets continue to be updated, added, and shared to augment the baseline verification metrics. The creation and on-line archival of weather forecast performance data metrics by the weather data centers makes the information available to irrigation decision tool developers.

Hollis, OK Mesonet Field Site

We use mesonet atmospheric and soil profile data from the Oklahoma Mesonet (McPherson, et al. 2007) at Hollis, OK (3 miles west of Gould, OK in Harmon County, OK) 34° 41' 7" N, 99° 49' 59" W). A site description for Hollis, OK indicates that its soil has a clay soil texture (44-56% clay) with relatively low native vegetation (OK Climatological Survey: Accessed August 19, 2019, http://www.mesonet.org/index.php/sites/site_description/holl). The OK Mesonet data for Hollis, OK is available on-line (OK Climatological Survey: Accessed August 19, 2019, http://www.mesonet.org/index.php/weather/category/soil_moisture ; Accessed August 19, 2019, http://www.mesonet.org/index.php/weather/category/soil_temperature) with additional data fields and variables for weather and climate also available. The soil moisture data is measured at 5, 25, and 60 cm depths every 30 minutes. Soil temperature data is available at 5 and 10 cm depths every 15 minutes for native vegetation, and at a 10 cm depth under bare soil. A

suite of meteorological sensor array data is available for the atmospheric measurements. The data that we use is from a September 2003 case study.

PREDICTIVE PROBABILITY METRIC RESULTS

We now intercompare and discuss predictive probability metrics using several examples. These metrics are later used to drive the land model sensitivity analysis results.

When interpreting the Threat Scores (TS) as a function of time it is important to recall that probabilities are being used to generate the TS, and that a perfect forecast of upcoming precipitation would receive a TS value of 1. Therefore, temporal differences are related linearly to probability improvements, so that a monthly (at a 0.5 in. (1.27 cm) precipitation threshold) TS value of 0.37 for the 1 Day June 2018 forecasts can be intercompared to the 2 and 3 Day TS values, 0.28, and 0.21, respectively (Fig. 1). The TS ratios can be used in irrigation tools like WISE to provide value and error estimation abilities using the precipitation forecast data. As perfect knowledge would have a TS value of 1, 1-TS is the amount that the forecasts will be degraded as each day progresses and the model error increases (to put it in a practical but negative light). Thus, from Figure 1, precipitation forecast results as derived 1-TS values at Day 1, 2, and 3 (+24h, +48h, and +72h forecast verification times) are: 63%, 72%, and 79% less likely to be correct than the verification observations at Day 0, as compared to just randomly selecting a chance rainfall event without any model assistance.

It is important to note in early spring, a critical soil moisture initial estimation period (Hook, 1994; Ceglar et al., 2017), that the forecasts are more accurate before the convective precipitation season begins. Thus, some decision-critical moments might be very well served by use of model estimates of precipitation as decisions are made in the early season, and also as light water application amounts are required (as the light rainfall events are also better predicted by the precipitation forecast systems). For the WPC-provided results shown in Fig. 1, the assessment of April 2018, has monthly TS values of 0.54, 0.49, and 0.45, respectively for forecast Days 1, 2, and 3. The TS values translate to improved (smaller) probability decreases of: 46%, 51%, and 55%, respectively. There is a ~ 40% prediction improvement in April as compared to June, which is in the more difficult convective precipitation seasonal forecast period for the continental United States. As there is substantial seasonality, it is important for irrigation management tools to understand the value of the precipitation forecasts for their particular crop

season, also conservative estimates can be used for the TS values (including the BIAS) which are also available at the same WPC web site. It should be noted however that the BIAS is targeted for minimization and mitigation by the WPC weather model development teams, as it can be mitigated using numerical techniques, while forecast skill is a predictive model performance element that is eventually overcome by increasing weather model errors at longer predictive times. Fig. 1 shows the progression of the model error increasing (with decreasing TS values) as it moves from Day 1 (red), to Day 2 (green), to Day 3 (blue). At some point in time the forecast stops having tangible value to the user (approaches a TS of zero). However, from a decision-making perspective, TS values above zero are likely where the costs and opportunity costs of deferring irrigation applications may lose value, as false rainfall predictions would force crops to endure dry conditions needlessly.

Increasing the precipitation threshold for the TS metric (for example using TS precipitation thresholds of 0.5 in (1.27 cm) to 1.0 in (2.54 cm) by intercomparing results shown in Figs. 1 and 2) tends to lower the TS values, as larger precipitation is associated with convective rainfall which is more non-linear and difficult to predict, especially in terms of spatial placement. While some radar data assimilation systems can improve the 0-12 h convective rainfall forecasts, it is very difficult to extend the error reductions into longer time periods due to the non-linear model error growth related to convective processes (Tai et al., 2011). The non-linearity model error growth problem also adversely impacts cloud-prediction at longer-predictive times in the satellite cloud data assimilation systems as well (e.g., see Vukicivic et al., 2004).

The interannual variability of the precipitation TS metrics can be significant. Here we compare 1.0" rainfall TS threshold results from June 2017 – June 2018 (Fig. 2) to June 2018 – June 2019 (Fig. 3). The June 2018 – June 2019 year was generally better predicted with a stronger winter (December and January) maximum of TS values than for the June 2017 – June 2018 year results. However, performance was degraded in the Fall of 2018 (September and October 2018) and the Spring of 2019 (March and April 2019) (Fig. 3) as compared to the 2017-2018 TS results (see Fig. 2). Thus, use of static TS results from one year to another for irrigation scheduling tool development could result in erroneous estimates of model performance as interannual precipitation variability is conditional on occurring weather conditions and synoptic and climatological dynamical flows (Gutzler, 2004). Model error biases can be manifested more

clearly in particular climatic regimes such as drought and monsoon periods (Novak et al., 2014). Thus, we recommend that model performance metrics be used that are appropriate for the current analysis season and region of interest.

The monthly NOAA WPC GFS BIAS results for June 2018 to June 2019 are shown in Fig. 4. Recall that a perfect BIAS score is one. As can be seen in Fig. 4, the model generally performs better in the winter than during the convective summer season (June – August). The BIAS also has a dependence with forecast lead times (see Day 1 (red), Day 2 (green), and Day 3 (blue) in Fig. 4) with generally shorter lead times having improved BIAS, however some longer-term forecasts (in the average) have improved BIAS statistics which indicates better statistical behaviors about not over- or under-predicting rainfall events. In practice the BIAS errors can be improved by applying Model Output Statistics (MOS) to adjust the BIAS of forecasts (Novak et al., 2014).

BS values can be similarly interpreted as the TS example above, keeping in mind that the computation of BS is different due to the use of the ensemble models, and that the BS is quadratic in terms of the probabilities, and thus should be interpreted by taking the square-root of the BS values (compare (1) and (3)). Also, since the total number of forecasts, n , is a scalar in the BS expression, BS values should only be interpreted with other like-computed BS values, and not intermixed with the TS values, as they are inherently different definitions: a perfect prediction BS score would tend toward zero in a quadratic manner with the rainfall prediction error, while a perfect prediction TS score tends toward 1 in a linear relationship with the rainfall prediction error. For example, in Fig. 5 the NOAA WPC GFS monthly precipitation forecast Brier Scores (BS) for July 2018 – July 2019 are shown. The BS results (Fig. 5) show the progression of the BS model error increasing (with increasing precipitation errors) as it moves from Day +3 (red), to Day +4 (green), to Day +5 (blue), to Day +6 (yellow), to Day +7 (orange). All results (Fig. 5) show similar increasing errors with greater prediction times for each month between July 2018 and July 2019. It is notable that the results for Feb. 2019 appear to perform worse in general than the other months for this particular monthly time series. This is likely caused by difficult intraseasonal/climatic conditions encountered during that month (Novak et al., 2014). Also note the relatively high BS values that are greater than 0.15 for predictive Days 6 and 7 (recall that it is quadratic in terms of precipitation errors, thus a BS of 0.1 is 22% more accurate than a forecast with a BS of 0.15, and 41% more accurate than a forecast with a BS of

0.2). This translates to relatively modest-to-poor rainfall prediction capabilities at Days 6-7. Thus, we anticipate that the TS values for predictive Days 1-3 would be more useful to actual irrigation scheduler tool users (as these shorter-term weather predictions are more accurate) depending on their time scale of interest. This demonstrates the trade-offs between seeking longer-term predictive capabilities, and the reduced accuracy of such predictions.

TIME-SCALE DEPENDENT RESULTS

Data assimilation methodologies can be used to provide insight into the links between model physics behaviors as a function of space and time when adjoints are used as a diagnostic tool. Adjoints of a tangent-linear model are used to efficiently compute local gradients of a function of model input and output parameters (Benedetti, et al. 2003). Using variational data assimilation methods, the optimization problem using adjoints of a tangent-linear model is normally focused on the reinitialization of the model state variables to minimize a penalty function in space and time (also known as a cost function) (Jones et al., 2019; Fletcher, 2017). In time-dependent variational techniques such as four-dimensional variational (4DVAR) data assimilation, the cost function can be determined as a function of the temporally-integrated adjoint sensitivities (Fletcher, 2017). Here we examine the linkage between space and time using adjoints of a vertical soil profile land model in an adjoint sensitivity analysis. In our case, the control variables are the soil moisture at various soil depths. The adjoint sensitivities, $\mathbf{L}(t_i, t_0)^T$, are computed with respect to these control variables, where \mathbf{L} is the tangent linear operator of the forward model, \mathbf{M} . The non-linear forward model in this case is a prognostic model of the energy and water fluxes within the vertical soil profile as a function of time and space and is based on the Land Ecosystem-Atmospheric Feedback model (LEAF-2) formulation (Walko, et al., 2000).

In our example the adjoints are computed for a single column, thus collapsing the 4DVAR system to a 2DVAR system. The land surface model and its respective adjoint sensitivities are used in a 2DVAR solver. Here we use a Gaussian 4DVAR framework (but applied to 2-dimensions (2D), i.e., vertical soil depth, z , and time, t); however, in the future, a non-Gaussian 4DVAR framework (Fletcher, 2017) could be used since soil moisture variables have skewed data distributions and are therefore non-Gaussian. Each of the 2DVAR model and adjoint components has undergone a series of tests (outlined in Jones et al., 2004). Here the work

differs from Jones et al. (2004), in that the temporal soil model variables as a function of depth are being analyzed rather than the microwave radiance operator adjoint sensitivities. In addition to perturbation-scaling-factor analysis (examined in detail in Jones et al., 2004) to gain physical insights into the model sensitivities for a range of parameters, nonlinear tests can be performed to ensure that the adjoints are correctly formulated and are operating within nominal linear regimes. The non-linear test is computed using linear inner product perturbation tests such that

$$NL = \frac{\langle L^T Lx', x' \rangle - \langle Lx', Lx' \rangle}{\langle Lx', Lx' \rangle}, \quad (4)$$

where $\langle \rangle$ denotes the inner product of the vectors, and x' is the model perturbation state vector. In the irrigation system use case, the model perturbation state vector contains a vector of rainfall perturbations and supporting land model environmental perturbation states, such as perturbations of soil moisture and soil temperature at a geographical site location. The NL test makes use of the fact that the two numerator expressions in (4) would be equal if the linear operator, L , were analytically linear. Our experience is that usually the NL test can be computed to within 1% accuracy for most encountered physical models, however each model could have its own unique challenges. Minimizing the problems encountered with strong non-linear systems may require redefining or constraining the strong nonlinearities or limiting the functions to their linear operating ranges.

A set of adjoint sensitivity tests can be conducted making use of the adjoint operators, the tangent linear model operators, and the perturbation vectors.

Figure 6 shows results from Hollis, OK, (just south of the Ogallala Aquifer Region (OAR) within western OK), assuming no additional rainfall after the initial rain event. Our results show that the penetration depth of the soil moisture information with time is dependent on soil texture information. Most soils show very deep penetration of the soil moisture sensitivity (>1 m soil depths) after approximately 1-2 weeks of temporal data assimilation (Fig. 6). However, some soils require longer integration times.

The adjoint sensitivity test estimates the relative component strength of the sensitivities of the soil moisture state vector in the vertical soil profile at 7 soil depths (-0.01, -0.02, -0.04, -0.08, -0.15, -0.30, -0.60, and -1.2 m depths). The adjoint-based relative component strength (RCS, after Jones et al., 2004) is given by

$$RCS_i = \frac{\langle L^T L x', x' \rangle_i}{\langle L^T L x', x' \rangle} \quad (5)$$

where $\langle \rangle_i$ denotes the inner product component of the i^{th} model vector element (e.g., the RCS_i component would correspond to the soil moisture variable, out of N possible model control variables in the model state vector, \mathbf{x}). The RCS_i measure is normalized to the full inner product, i.e., the denominator of (5), which is always positive. All RCS magnitudes for a particular base state sum to 100%, i.e.,

$$\sum_{i=1}^N RCS_i = 100\%. \quad (6)$$

In Figure 6 normalized adjoint sensitivity (i.e., RCS) results are shown for the soil moisture variables at each model soil level (7 soil levels are used here) as a function of adjoint integration time. It is important to note that the dependency of the RCS_i on a particular surface soil moisture perturbation (equivalent to a precipitation input flux) switches between the surface variables and the upper soil levels down toward the lower soil levels as the soil continues to dry out with time. The state variables are initialized with atmospheric station data from Hollis, OK (34° 41' 11" N, 99° 55' 1" W) from the Oklahoma Mesonet (McPherson et al., 2007). The soil begins the simulation integration using a soil-saturated volumetric soil moisture content, with the soil experiencing drying atmospheric conditions (however, the actual conditions are less important than the pedantic demonstration of the adjoint sensitivities, as any condition within the OAR could be evaluated using the relative component strength method).

The perturbation strength is initially very large for the near-surface soil layer (the -0.01 cm level – it is a shallow soil layer, so it has less water than the lower levels to diffuse toward the atmosphere via evapotranspiration). The sensitivity results show increasing times between alternating sensitivity leadership from the top to the lower soil moisture levels. The strength of the sensitivity decreases as the integration is performed, however since we are normalizing the component strengths, the adjoint sensitivity results can be used to instead demonstrate the sensitivity “leadership” as a function of time.

The perturbation strength analysis using the adjoint method demonstrates the power of the adjoint sensitivities, as it is computing the sensitivities using the adjoint and tangent linear operators without having to perform numerous Monte Carlo simulations, or other perturbation-based numerical system sensitivity studies, as the adjoint sensitivity study is performed as a

series of function calls. The analysis is also a fully simultaneous sensitivity analysis solution and could just as easily demonstrate joint perturbation effects with simultaneous multivariate perturbations being used instead of other perturbation analysis interactions.

From the results shown in Fig. 6, time scales up to 7-14 days should be considered for soil dry-down if roots penetrate to the 1.2 m soil depth. While alternate scenarios could be studied for differing solar, atmospheric, and cloud conditions to understand those effects, systems like the adjoint sensitivity analysis can demonstrate constraints on various scenarios and can help identify precipitation temporal windows of importance for particular crop growth stages (with root depths at various associated levels). As each depth has a unique time decay period, the time decay values could be used within the irrigation tools to better understand the value of the water that is being placed onto the crop at a particular time, thus helping to further prioritize the value of plant available water amounts.

SUMMARY AND CONCLUSIONS

Summary of Results

We applied several precipitation forecast verification metrics to the NOAA GFS model predictions (Novak, et al. 2014) for use with the irrigation scheduler optimization problem. We also applied the numerical weather prediction (NWP) data assimilation methodologies to a land model to demonstrate a method to diagnose adjoint sensitivities to address important prognostic water constraint questions, such as “how long can I delay a crop water application?”.

A commercial provider of GFS predictive weather data (aWhere, Inc. system. Accessed August 19, 2019: <https://www.aWhere.com>) is used to enable efficient near real-time access within a cloud-based framework. The precipitation verification metrics are available (monthly, seasonally, and regionally) in near real-time for use by the irrigation management research community for further prognostic weather data use within irrigation tool developments and research.

The following is a summary of key results:

(1) From the predictive probability metric results, seasonal precipitation forecast differences show enhanced abilities of the forecast data to perform well in early spring which is a critical period for soil moisture conditions for crop management decisions (Hook, 1994; Ceglar

et al., 2017). The GFS precipitation forecast verification results show a general decrease in predictive skill during the summer convective precipitation months.

(2) In addition, the prediction probability metric results show that precipitation forecast skills are stratified by precipitation threshold amount, with light rain events being forecast with more skill and heavy rainfall events being forecast with less skill.

(3) A time analysis of the predictive weather performance metrics show that as precipitation forecasts predict further into the future that their TS and BS values decrease; however, it is noted that economic and conservation values are determined by the particular crop application, and needs to be assessed within the context of the economic opportunity-costs of delaying an irrigation application. In addition, it was shown from the time series analysis that the presence of interannual variability within the predictive model rainfall performance results in a recommendation that current model performance metric statistics be used in irrigation scheduler tools to represent ongoing climatic and synoptic weather conditions.

(4) A time-scale dependent analysis using adjoint model sensitivities was demonstrated with a case study application at Hollis, OK. The adjoint sensitivity results are used to examine complex soil profile issues that are a function of meteorological data, soil conditions, and crop growth stage as a function of space and time. The adjoints are helpful to diagnose the question of “how long can I delay a crop water application”, as many simultaneous feedbacks are represented within the analysis. Adjoint model sensitivities are also shown to be computationally efficient and are used to integrate the atmospheric, soil, and crop conditions for effective near real-time agronomic decisions.

Current Status of the WISE System Development

The WISE system is publicly available (WISE. Accessed August 19, 2019, <http://wise.colostate.edu/>). The current system is operational using Colorado Agricultural Meteorological Network (CoAgMet) weather station data with predictive weather data from aWhere currently undergoing extensive offline tests. The adjoint sensitivities and uncertainty propagation is not yet integrated into WISE but rather is a standalone diagnostic tool. In the future, additional tests and assessments will determine if the adjoint sensitivities are fully integrated into the online operational WISE. Currently many studies are possible to examine use

of the adjoint sensitivity method to optimize various WISE model parameters to improve its performance. That work will be part of our next incremental WISE development steps.

Conclusions

Due to the availability of new data sets and data management capabilities, and the capacity of cloud-based software frameworks, numerous near real-time enhancements to WISE are possible. The weather performance metrics should be integrated into future irrigation tools, so that costs and decisions can be balanced adequately. Soon, we plan additional tests of the hypothesis that the prognostic NWP precipitation information adds value to WISE. We will also explore the limits of that information to improve decision-making. Selected irrigated fields in northeast Colorado that are near CoAgMet weather stations will be used to further test the integration of NWP precipitation forecasts with WISE for many additional crop management configurations and situations. We also plan to collaborate with OWCAP team members based at Kansas State University (KSU), Texas A&M, and Oklahoma State University (OSU) who are working to improve other related Ogallala-focused irrigation decision-support systems.

In conclusion, we have created a shareable test environment for linking irrigation tools to weather and climate to improve decision-making systems leading to optimized crop performance and yield. Many facets of irrigation decision-making could be impacted and targeted by specific optimization methods. For example, water efficiencies could be gained by optimizing water applications within time and space targeting crop growth stages and sensitivities to crop yield as a function of soil depth. Water and fertilizer costs could be optimized toward immediate water availability (perhaps due to upcoming scheduled water restrictions during drought conditions) and the economic opportunity risks of waiting for predicted rainfall, rather than continuing to apply water and fertilizer at times that might not be as optimal. These decision-making methods could also be used to estimate and minimize the probabilities of encountering increased costs due to fertilizer leaching effects. Thus, making fertilizer applications more cost effective as an active part of the irrigation management decision chain. Secondary effects such as reducing surface runoff from the over application of water could likewise be important to soil sustainability, limiting soil wind erosion, and improving downstream water quality. Healthy soils that balance soil moisture conditions with soil microbiome community development requirements could help mitigate soil fungal disease issues and improve overall soil health. All these potential benefits

could be through a series of balanced and optimized controlled water applications through intentional and comprehensive crop management practices. Looking ahead to the future, additional teams and networks-of-teams, along with industry partners, can build upon these multi-disciplinary and multi-faceted modeling capabilities, as demonstrated by the growing cadre of precision agriculture analytics firms that are driven by cloud-based data sets and services (Wolfert et al., 2017).

ACKNOWLEDGMENTS

Dr. Jones thanks Drs. Tarendra Lakhankar and Manajit Sengupta, and Mr. Gary McWilliams, for the many science discussions pertaining to the soil moisture adjoint sensitivity discussions. We gratefully acknowledge research funding support from the United States Department of Agriculture (USDA) National Institute of Food and Agriculture (NIFA) under award number 2016-68007-25066, “Sustaining agriculture through adaptive management to preserve the Ogallala aquifer under a changing climate”, and portions are based upon work supported by the National Science Foundation under Grant Number (1738206).

LITERATURE CITED

- Benedetti, A., G. Stephens, and T. Vukicevic, 2003. “Variational assimilation of radar reflectivities in a cirrus model. II: Optimal initialization and model bias estimation.” *Quarterly J. Royal Meteorological Society* 129 : 301-319, <https://doi.org/10.1256/qj.02.64>
- Brier, G.W. 1950. “Verification of forecasts expressed in terms of probability.” *Monthly Weather Review* 78 : 1-3. [https://doi.org/10.1175/1520-0493\(1950\)078<0001:vofeit>2.0.co;2](https://doi.org/10.1175/1520-0493(1950)078<0001:vofeit>2.0.co;2)
- Ceglar, A., M. Turco, A. Toreti, F.J. Doblas-Reyes. 2017. “Linking crop yield anomalies to large-scale atmospheric circulation in Europe.” *Agricultural and Forest Meteorology* 240-241 : 35-45, <https://doi.org/10.1016/j.agrformet.2017.03.019>
- Charba, J.P., and F.G. Samplatsky. 2011. “High-resolution GFS-based MOS Quantitative Precipitation Forecasts on a 4-km Grid.” *Monthly Weather Review* 139 : 39-68, <https://doi.org/10.1175/2010MWR3224.1>

- Fletcher, S.J. 2017. *Data Assimilation for the Geosciences: From Theory to Application*. Elsevier: Amsterdam, The Netherlands, 976 pp. <https://doi.org/10.1016/B978-0-12-804444-5.00001-5>
- Gutzler, D.S. 2004. "An index of interannual precipitation variability in the core of the North American Monsoon Region." *Journal of Climate* 17 : 4473-4480, <https://doi.org/10.1175/3226.1>
- Hamill, T.M., E. Engle, D. Myrick, M. Peroutra, C. Finan, and M. Scheuerer. 2017. "The U.S. National Blend of Models for the statistical postprocessing of probability of precipitation and deterministic precipitation amount." *Monthly Weather Review* 145 : 3441-63. <https://doi.org/10.1175/MWR-D-16-0331.1>
- Hook, J.E. 1994. "Using crop models to plan water withdrawals for irrigation in drought years." *Agricultural Systems* 45 (3) : 271-289. [https://doi.org/10.1016/0308-521X\(94\)90142-3](https://doi.org/10.1016/0308-521X(94)90142-3)
- Jones, A.S., T. Vukicevic, and T.H. Vonder Haar. 2004. "A microwave satellite observational operator for variational data assimilation of soil moisture." *Journal of Hydrometeorology* 5 : 213-29. [https://doi.org/10.1175/1525-7541\(2004\)005<0213:AMSOOF>2.0.CO;2](https://doi.org/10.1175/1525-7541(2004)005<0213:AMSOOF>2.0.CO;2)
- Jones, M.S., B.A. Colle, and J.S. Tongue. 2007. "Evaluation of a mesoscale short-range ensemble forecast system over the northeast United States." *Weather and Forecasting* 22 : 36-55. <https://doi.org/10.1175/WAF973.1>
- Jones, A.S., A. Andales, J.L. Chávez, C. McGovern, G.E.B. Smith, O. David, and S.J. Fletcher. 2019. "Use of predictive weather uncertainties in an irrigation scheduling tool Part I: A review of metrics and adjoint methods." *Journal of American Water Resources Association*, (this issue).
- Marty, R., I. Zin, C. Obled, G. Bontron, and A. Djerbgua. 2012. "Toward real-time daily PQPF by an analog sorting approach: Application to flash-flood catchments." *Journal of Applied Meteorology and Climatology* 51 : 505-20. <https://doi.org/10.1175/JAMC-D-11-011.1>
- McPherson, R.A., C. Fiebrich, K.C. Crawford, R.L. Elliott, J.R. Kilby, D.L. Grimsley, J.E. Martinez, J.B. Basara, B.G. Illston, D.A. Morris, K.A. Klosel, S.J. Stadler, A.D. Melvin, A.J. Sutherland, and H. Shrivastava, 2007: "Statewide monitoring of the mesoscale environment:

A technical update on the Oklahoma Mesonet.” *Journal of Atmospheric and Oceanic Technology* 24 : 301-21. <https://doi.org/10.1175/JTECH1976.1>

Novak, D.R., C. Bailey, K.F. Brill, P. Burke, W. A. Hogsett, R. Rausch, and M. Schichtel. 2014. “Precipitation and temperature forecast performance at the Weather Prediction Center.” *Weather and Forecasting* 29 : 489-503. <https://doi.org/10.1175/WAF-D-13-00066.1>

Rogers, D.H., and M. Alam. 2007. *KanSched2 – An ET-based irrigation scheduling tool users guide*. Kansas State University Research Extension. Electronic publication only. EP-12. 12pp. Available at <https://core.ac.uk/download/pdf/33360304.pdf>

Tai, S.-L., Y.-C. Liou, J. Sun, S.-F. Chan, and M.-C. Kuo. 2011. “Precipitation forecasting using doppler radar data, a cloud model with adjoint, and the weather research and forecasting model: Real case studies during SoWMEX in Taiwan.” *Weather and Forecasting* 26 : 975-992. <https://doi.org/10.1175/WAF-D-11-00019.1>

Vukicevic, T., T. Greenwald, M. Zupanski, D. Zupanski, T. Vonder Haar, and A.S. Jones. 2004. “Mesoscale cloud state estimation from visible and infrared satellite radiances.” *Monthly Weather Review* 132 : 3066-3077. <https://doi.org/10.1175/MWR2837.1>

Walko, R.L., L.E. Band, J. Baron, T.G.F. Kittel, R. Lammers, T.J. Lee, D. Ojima, R.A. Pielke, C. Taylor, C. Tague, C.J. Tremback, and P.L. Vidale, 2000. “Coupled Atmosphere-Biophysics-Hydrology Models for Environmental Modeling.” *J. Applied Meteorology* 39 :931-944, [https://doi.org/10.1175/1520-0450\(2000\)039<0931:CABHMF>2.0.CO;2](https://doi.org/10.1175/1520-0450(2000)039<0931:CABHMF>2.0.CO;2)

Wolfert, S., L. Ge, C. Verdouw, and M.-J. Bogaardt. 2017. “Big Data in smart farming – A review.” *Agricultural Systems* 153 : 69-80. <https://doi.org/10.1016/j.agsy.2017.01.023>

Xia, Y., M.B. Ek, Y. Wu, T. Ford, S.M. Quiring. 2015. “Comparison of NLDAS-2 simulated and NASMD observed daily soil moisture, Part I: Comparison and analysis.” *Journal of Hydrometeorology* 16 : 1962-80. <https://doi.org/10.1175/JHM-D-14-0096.1>

LIST OF FIGURES

Figure 1. National Oceanographic and Atmospheric Administration (NOAA) Weather Prediction Center (WPC) Global Forecast System (GFS) monthly precipitation forecast Threat Score (TS) for June 2017-June 2018 for a 0.5 in. (1.27 cm) precipitation threshold. Data results are from the monthly WPC verification (WPC verification system. Accessed July 15, 2018,

<https://www.wpc.ncep.noaa.gov/images/hpcvrf/wpc10.gif>). The TS for a 0.5 in. (1.27 cm) precipitation threshold is shown for lead times of (red) Day 1 (+24h), (green) Day 2 (+48h), and (blue) Day 3 (+72h).

Figure 2. NOAA WPC GFS monthly precipitation forecast TS for June 2017-June 2018 for a 1.0 in. (2.54 cm) precipitation threshold. Data results are from the monthly WPC verification (WPC verification system. Accessed July 15, 2018,

■ <https://www.wpc.ncep.noaa.gov/images/hpcvrf/wpc10.gif>). The TS for a 1.0 in. (2.54 cm) precipitation threshold is shown for lead times of (red) Day 1 (+24h), (green) Day 2 (+48h), and (blue) Day 3 (+72h).

Figure 3. NOAA WPC GFS monthly precipitation forecast TS for June 2018-June 2019 for a 1.0 in. (2.54 cm) precipitation threshold. Data results are from the monthly WPC verification (WPC verification system. Accessed August 16, 2019,

<https://www.wpc.ncep.noaa.gov/images/hpcvrf/wpc10.gif>). The TS for a 1.0 in. (2.54 cm) precipitation threshold is shown for lead times of (red) Day 1 (+24h), (green) Day 2 (+48h), and (blue) Day 3 (+72h).

Figure 4. NOAA WPC GFS monthly precipitation forecast Bias (BIAS) for June 2018-June 2019 for a 1.0 in. (2.54 cm) precipitation threshold. Data results are from the monthly WPC verification (WPC verification system. Accessed August 16, 2019,

<https://www.wpc.ncep.noaa.gov/images/hpcvrf/wpc10bias.gif>). The Bias for a 1.0 in. (2.54 cm) precipitation threshold is shown for lead times of (red) Day 1 (+24h), (green) Day 2 (+48h), and (blue) Day 3 (+72h).

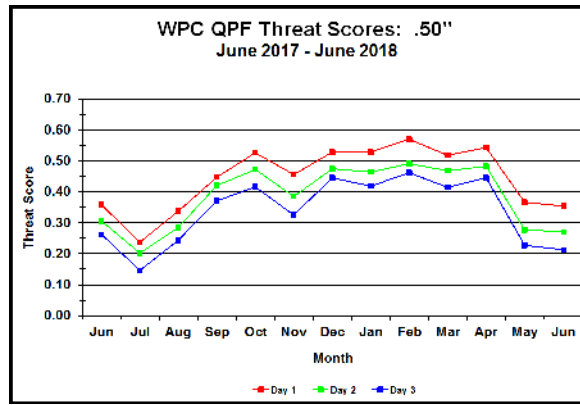
Figure 5. NOAA WPC GFS monthly precipitation forecast Brier Scores (BS) for July 2018-July 2019 for forecast days 3-7. The monthly composite is valid for the analysis date (listed on the abscissa as Year/Month). Data results are from the monthly WPC verification (WPC verification system. Accessed August 16, 2019,

■ <https://www.wpc.ncep.noaa.gov/images/hpcvrf/brier.gif>). The BS are for precipitation forecast lead times of (red) Day 3 (+72h), (green) Day 4 (+96h), (blue) Day 5 (+120h), Day 6 (+148h), and Day 7 (+172h).

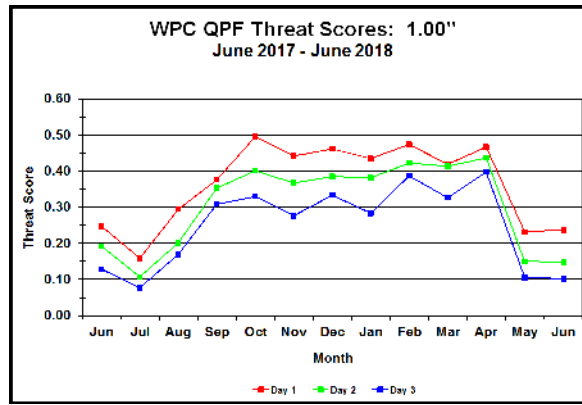
Figure 6. Normalized adjoint sensitivity results for Hollis, Oklahoma soil conditions for a Sep. 2003 case study. Soil depths are (blue) -0.01 m, (green) -0.02 m, (dark red) -0.04 m, (purple) -0.08 m, (light blue) -0.15 m, (yellow) -0.30 m, (magenta) -0.60 m, and (dark blue) -1.2 m, as a

function of adjoint integration time (adjoint integration times move from right to left, integrating back to the initial soil moisture conditions at time, t_0 . Maximum depth sensitivity at a 1.2 m depth (highlighted above) is achieved after 14 days of adjoint integration backwards in time (at $t=7$ days).

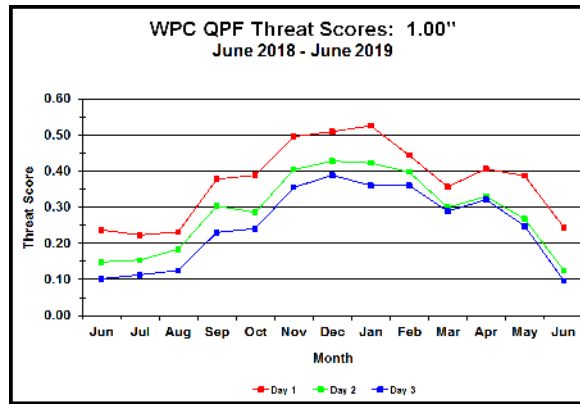
Author Manuscript



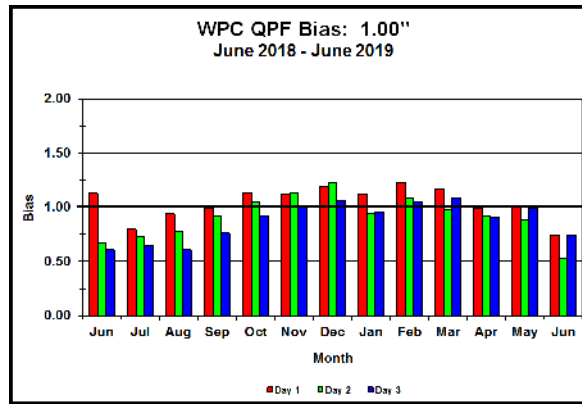
jawra_12806_f1.tif



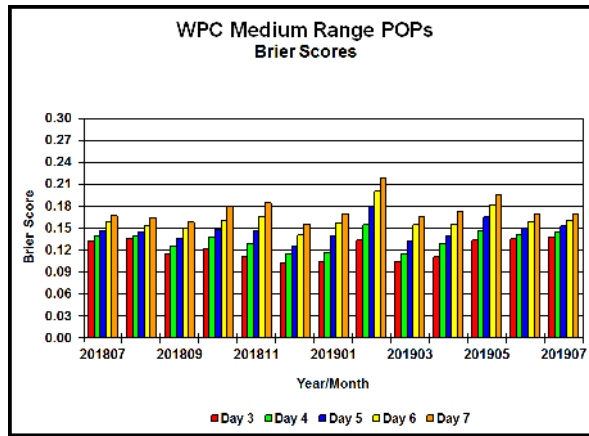
jawra_12806_f2.tif



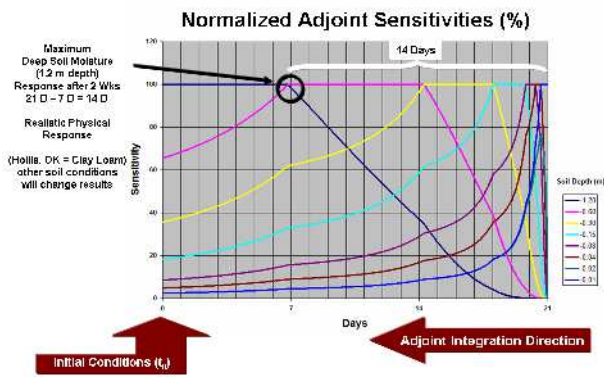
jawra_12806_f3.tif



jawra_12806_f4.tif



jawra_12806_f5.tif



jawra_12806_f6.tif